Proceedings of the Fourth International Symposium
on
ADVANCED NUCLEAR ENERGY RESEARCH
— *ROLES AND DIRECTION OF MATERIAL SCIENCE IN NUCLEAR TECHNOLOGY*—

STUDIES ON SILICON, METALS, AND CARBON CLUSTERS

Shigeo Maruyama
Department of Mechanical Engineering,
The University of Tokyo
7-3-1 Hongo, Bunkyo-ku, Tokyo 113, Japan
Phone 03-3812-2111 ext. 6421 Fax 03-3818-0835

Abstract: A miniaturized pulsed supersonic beam source has been developed using laser vaporization of a computer-controlled target disk, producing intense beams of cluster ions with excellent repeatability and control. This source is directly attached to a Fourier transform ion cyclotron resonance (FT-ICR) apparatus. With this new configuration, FT-ICR studies of various clusters such as silicon, metals, and carbon are accomplished. From these experiments, interesting features of these clusters are summarized. Special emphasis is on laser annealing of geometrical isomers of silicon clusters and metal clusters while they are levitated in the ICR cell. The photofragmentation experiments of giant fullerenes, ranging from C_{150} to C_{600}, and thermionic emission from them are also featured.

Key Words: Cluster, FT-ICR, Mass spectrum, Laser vaporization, Supersonic nozzle, Chemical reaction, Silicon, Transition metals, Carbon, Fullerene.

1. INTRODUCTION

Clusters of 2 to about 1000 atoms of semiconductor materials, metals, or carbon have quite different properties from the bulk solid or the isolated single atom. Under certain conditions, however, it will be possible to use these clusters as simple models of bulk surface sciences. Or, interesting properties of certain small clusters will be a nice exercise of quantum calculations. In addition to the theoretical interest, such clusters may play an important role in making thin films by vapor deposition techniques. Furthermore, studies of such clusters may lead to findings of materials of completely new form such as C_{60} now widely known as Buckminsterfullerene.

Experimental studies of those clusters are performed using a newly designed supersonic cluster beam source (mini-source) and a FT-ICR spectrometer. In the cluster source, a computer-controlled target disk of solid material is vaporized by a focused laser light and is cooled and carried by a timed helium gas pulse. Due to small size of the chamber and narrow pulse width, entire source is adequately pumped by a single 170 l/s turbopump. This vacuum quality permits the direct connection of the source to the FT-ICR apparatus. Hence, it turned out to be the smallest external ion source for FT-ICR apparatus.

Cluster beam is directly injected to a 6 Tesla superconducting magnetic field of the FT-ICR part of the apparatus. While cluster ions are trapped and levitated in the ultra-high vacuum of FT-ICR for a many minutes, desired combinations of computer-controlled procedures such as thermalization, mass selection, chemical reaction, laser irradiation, and thereafter detection of mass spectrum can be done.

Reaction studies of ethylene on silicon confirmed that silicon cluster with certain number of atoms are far less reactive than others. Those silicon clusters of magic numbers were found to have more than two isomers with vastly different reactivity. Then, it was demonstrated that those clusters can be annealed to a single geometrical form by excimer laser irradiation followed by collisional cooling while they are levitated in the ICR trap. This laser annealing technique is also applied to the transition metals. Finally, giant fullerenes up to C_{600} are proved in the FT-ICR apparatus.

2. CLUSTER MINI-SOURCE

Fig. 1 displays a schematic cross section of the new compact cluster beam source [1]. It is based on laser vaporization of a rotating, translating target surface mounted on the front of a pulsed supersonic valve. As shown in Fig. 1, whole source fits in a single 6" six-way UHV cross. Six flanges hold fast pulsed valve of helium, window for the vaporization laser, target disk mount mechanism, skimmer, turbopump (bottom), and view-window (top). The design philosophy is that it is best to fire the vaporization laser on the leading edge of the rising carrier gas pulse. Otherwise a well-defined shock wave forms in the high-density carrier gas above the target as the laser vaporized plume begins to expand. The confinement of the plume will result the large scale condensed solid particle leaving only a tiny amount of medium size clusters. In order to sufficiently cool the clusters without confining the vaporized plume, an extremely fast-rising pulsed nozzle was employed. The vaporizing laser is fired at the leading edge of the gas pulse. The magnetic "current loop" type pulsed supersonic valve used is now commercially available from R. M. Jordan Company.

For the experiments reported here the vaporization laser pulse (Nd: YAG 2nd harmonic, typically 10 mJ per shot) was focussed to a spot 0.7 mm diameter and reached the target disk through a 1 mm diameter hole in the nozzle block. Exit of the fast pulsed valve is connected to a cylindrical space labeled "waiting room" in Fig. 1. This waiting room is designed so that the helium gas will swirl and establish the certain repeatable pressure at the time of laser vaporization. Details of dimensions of the nozzle available in the earlier publication [1] is crucial for the performance of this mini-source.

The target disk is rotated and translated with two computer controlled stepping motors in order to vaporize the small disk evenly. And, when an adjustment of the alignment of the vaporization laser is needed, the target disk will translate out of way so that the laser beam passes through the nozzle block and the small window on the disk-mount flange. Precise alignment is then easily achieved by monitoring the shape of the transmitted laser beam.

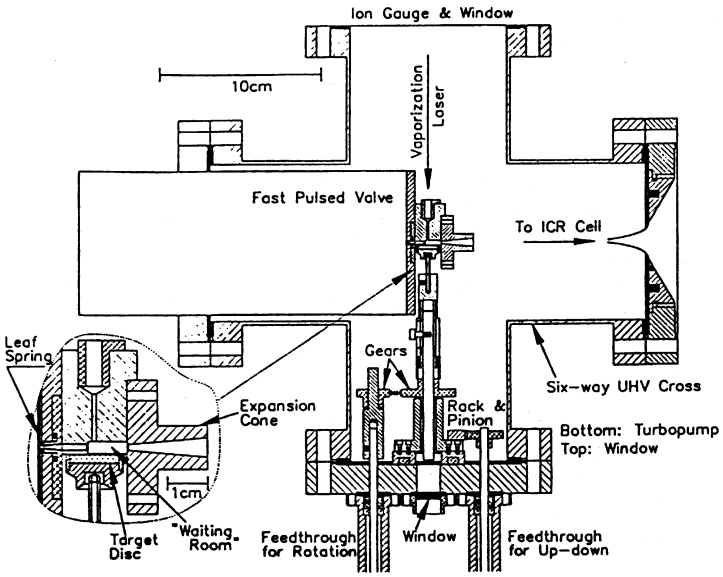

Fig. 1. Cluster Mini-source [1]. The compact pulsed supersonic cluster beam source using laser vaporization of a target disk that is rotating and translating under computer control.

For this small size and using a short pulse of helium carrier gas (30 μm), a single 170 l/s turbopump is sufficient to adequately pump the chamber. The resultant vacuum quality permits the direct connection to the FT-ICR apparatus.

3. FT-ICR

Cluster beam generated in the mini-source is aimed directly down the central axis of the 6 Tesla superconducting magnet of the FT-ICR apparatus, which is schematically displayed in Fig. 2 [1,2]. The ICR trap was centered in the homogeneous region of the magnetic field where the radial ion motion was confined by the magnetic Lorentz force which determines the cyclotron motion. Along the magnetic central axis the confinement of the cluster ions in the trap was accomplished by two conical-shaped electrodes -- the "front" and "back" doors labeled in Fig. 2. Note that the doors had large (2.5 cm i.d.) holes in the center to permit the clusters to pass through whenever permitted by their axial energy. These holes also allowed free passage of laser radiation without scattering. The side plates of the ICR trap were composed of four sectors of a 4.8 cm i. d. cylinder, 15.0 cm in length. Two opposing 120° were used for rf excitation of the trapped cluster ions, while the other two 60° sectors were used for detection of the image current induced by the cyclotron motion.

In front of the "front" door was a "screen" door that was mounted close to a two-part tubular structure labeled the "deceleration tube." These two parts of the deceleration tube were connected together by a flexible wire and to an external voltage pulser through a connection at the source

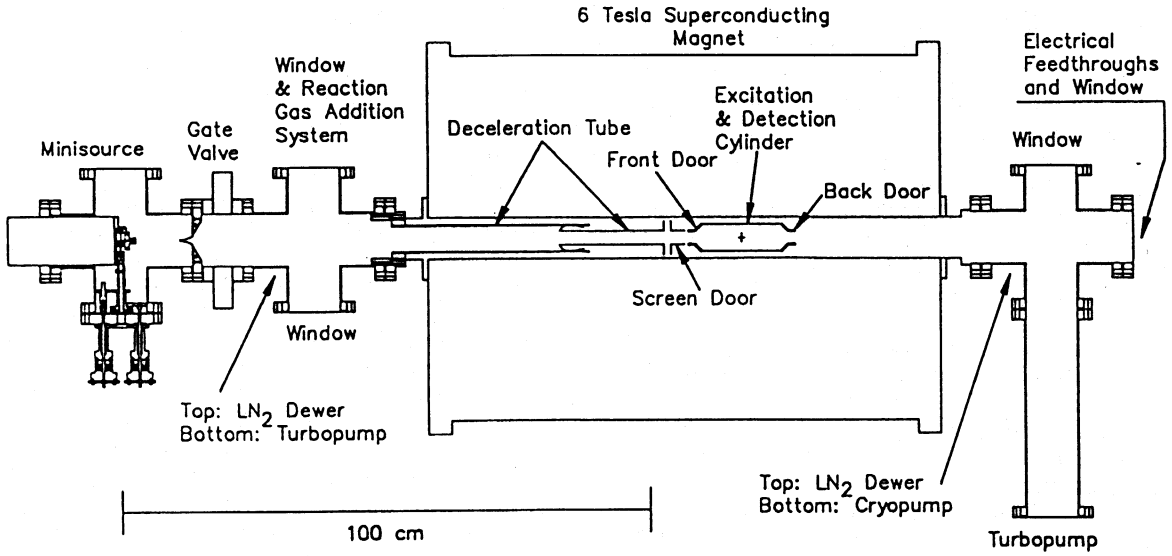

Fig. 2. Schematics of FT-ICR apparatus with direct connection to the mini-source [1].

side. Positively charged clusters traveling through the middle of this tube were effectively decelerated as they passed on the "screen" door because the decelerator tube was pulsed to a negative potential while they were still inside and experienced no field in this nearly closed conductor before they attempted to "climb out" of the decelerator tube to get back to ground potential at the screen door.

As shown in Fig. 2, entrance and exit to the bore tube of the FT-ICR magnet was connected to two 6" six-way crosses, each of which was pumped by a separate 170 l/s turbopump. In addition, the last cross was pumped by a 20 cm i.d. CTI cryopump that was valved off under computer control by a single-vane butterfly valve during the injection cycle. Ordinally, for experiments reported here the pressures recorded near these six-way crosses on either side of the FT-ICR bore tube when cluster beam source was off were in low 10^{-9} Torr range.

Fig. 3 displays a typical FT-ICR mass spectrum of positive cluster ions directly injected using the new source with a germanium target disk. For this experiment, ionization is only the residual amount left after recombination of the original laser-induced plasma. For the bulk of the ICR experiments of interest with positive and negative clusters, this mode of using the residual ionization from the laser vaporization event is quite adequate.

Since the germanium cluster ions are all accelerated to nearly the same 1.9×10^5 cm/s velocity by the supersonic expansion, each cluster has a translational energy that is linearly dependent on its mass. This fact permits a coarse selection of the range of clusters to be trapped in the ICR cell simply by controlling the deceleration voltage. In the example shown in Fig. 3 the deceleration tube was pulsed to -45 V after a 450 μs delay from the vaporization laser pulse to allow the clusters sufficient time to pass deep into the tube while it was still at ground potential. As the cluster ion packet neared the end of the deceleration tube 110 μs later, the screen door was pulsed from 10 V down to 0 V and held there for 80 μs, allowing the cluster ion packet to pass through as decelerated. During the injection cycle the front and back doors are held at 4 V and 10 V, respectively.

In order to produce the mass spectrum of Fig. 3, the injection process was repeated 10 times over a period of 1 s. After the injection process the front and back door voltages were ramped to 10 V over a period of 1.0 s, and the clusters were then exposed to argon at a pressure of 2×10^{-5} Torr for 2-10 s in order to thermalize their motions in the ICR trap to near 300 K. The ICR transient was then excited with a computer-generated rf waveform having constant power over the frequency range of interest and resulting coherent ICR transient was detected and processed to produce the spectrum shown in Fig. 3.

Due to the many isotopes of germanium with substantial natural abundance there is quite an extensive range of masses present in the ICR cell as injected from the supersonic beam. As is evident in Fig. 3 these isotopomers leave very little baseline between peaks for adjacent clusters on which to look for reaction products. As seen in the top panel of Fig. 4, this initial distribution may be dramatically simplified by selectively sweeping some of the clusters from the cell. This technique, commonly known as "SWIFT" (stored waveform inverse Fourier transform), involves the calculation of the inverse Fourier transform of the rf power spectrum needed to sweep selected ions from the ICR cell. The resulting time domain waveform is then generated by a fast 14-bit DAC, amplified and applied to the rf excitation plates of the ICR cell. In the case of Fig. 4 this SWIFT waveform was chosen so as to sweep out a clean baseline between the dominant isotopic components

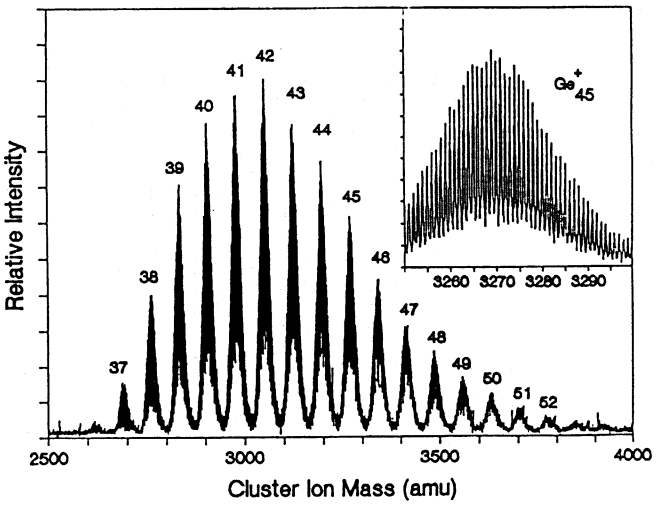

Fig. 3. FT-ICR mass spectrum of Ge clusters [1]. The insert panel is an expanded view showing the isotopic substructure of the Ge_{45}^+ clusters.

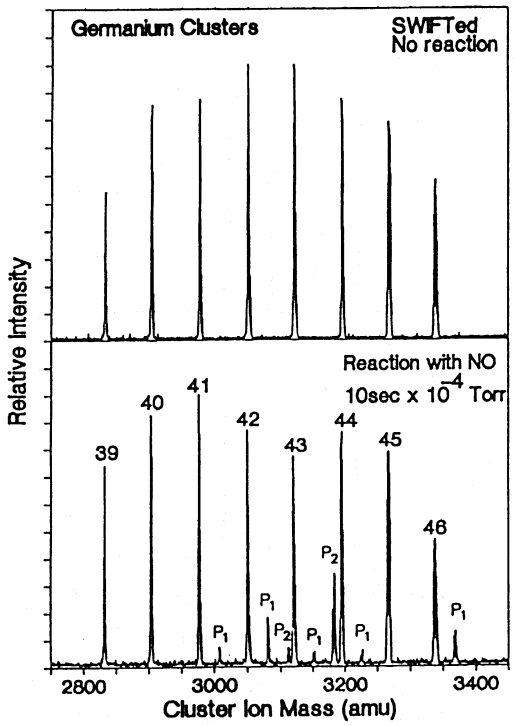

Fig. 4. Reaction study of Ge_n^+ clusters with nitric oxide [1]. The top panel shows the FT-ICR mass spectrum after selectively removal of some ions from the cell by "SWIFT" excitation. The bottom panel shows this spectrum after exposure to 1×10^{-4} Torr nitric oxide for 10s. Reaction product of the form $Ge_n(NO)_m^+$ are labeled as "P_m".

of the germanium clusters in the 39–46 atom size range.

The bottom panel of Fig. 4 shows the result of exposure of the selected clusters to nitric oxide gas at a pressure of $1x10^{-4}$ Torr for 10 s. Prior to the reaction the clusters had been thermalized to 300 K by roughly 2000 collisions with argon. For some clusters such as Ge_{43}^+ reaction products of the form $Ge_{43}NO^+$ and $Ge_{43}(NO)_2^+$ are clearly seen, whereas other clusters such as Ge_{39}^+ and Ge_{45}^+ show no evidence of reaction at all.

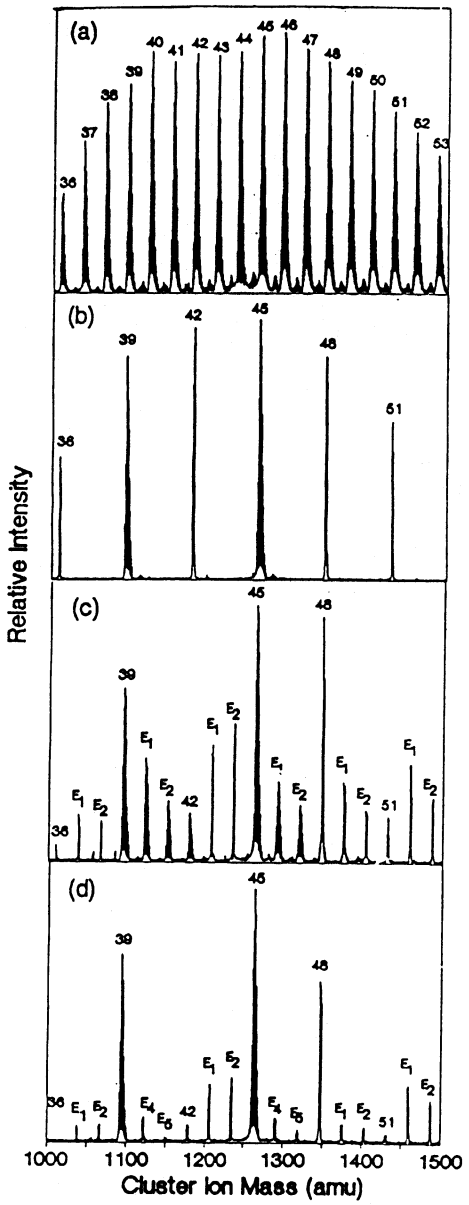

Fig. 5. Ethylene chemisorption and laser annealing study of silicon clusters [4]. (a) Mass spectrum of Si_n^+ clusters as injected from the mini-source. (b) After the "SWIFT" excitation. (c) After exposure to $1x10^{-5}$ Torr ethylene for 20 s. (d) The same reaction experiments as panel (c) except that the clusters were annealed prior to reaction by irradiation with 30 pulses of XeCl excimer laser at 10 Hz at a fluence of 1 mJ/cm^2 per pulse followed by a 3 s thermalization collision with $2x10^{-5}$ Torr argon.

4. SILICON CLUSTERS

The positively charged clusters of silicon with 21, 25, 33, 39, and 45 atoms were found to be relatively unreactive toward chemisorption of ammonia or ethylene, while clusters with only one atom more or less reacted rapidly [2,3]. This striking observation led to the suggestion that silicon clusters in this size range may adopt special geometrical forms. If small clusters of such elements as silicon are to be useful as a model of the surface chemistry of the bulk, it will be necessary to find a reliable way to anneal them to a well-defined structure. Here, the evidence that such annealing is possible through the use of laser excitation of the clusters levitated in the magnetic field of a FT-ICR spectrometer [4].

Fig. 5 gives an example of the critical data for this experiment. The top panel (a) displays the FT-ICR mass spectrum of silicon clusters in the 36–53 atom size range as injected from the mini-source. In this case the injection process was repeated for 100 cluster beam pulses at a rate of 10 Hz in order to adequately fill the ICR trap. Following the similar SWIFT procedure as the case of germanium in Fig. 4, the second panel of Fig. 5 (b) is obtained. In this case, however, the SWIFT excitation was chosen such that different isotopic widths were left for each cluster size remaining in the ICR trap. The third panel of Fig 5 (c) shows the result of exposure of these selected clusters to ethylene at $1x10^{-5}$ Torr for 20 s. Note that in this case the isotopic width does serve as a nice tracer of the parentage of each reaction product. As described before [3], ethylene chemisorption on these silicon cluster is somewhat selective. As seen in panel (c) Si_{39}^+, Si_{45}^+, and Si_{48}^+ appear a bit less reactive than the other clusters, but it is clear that

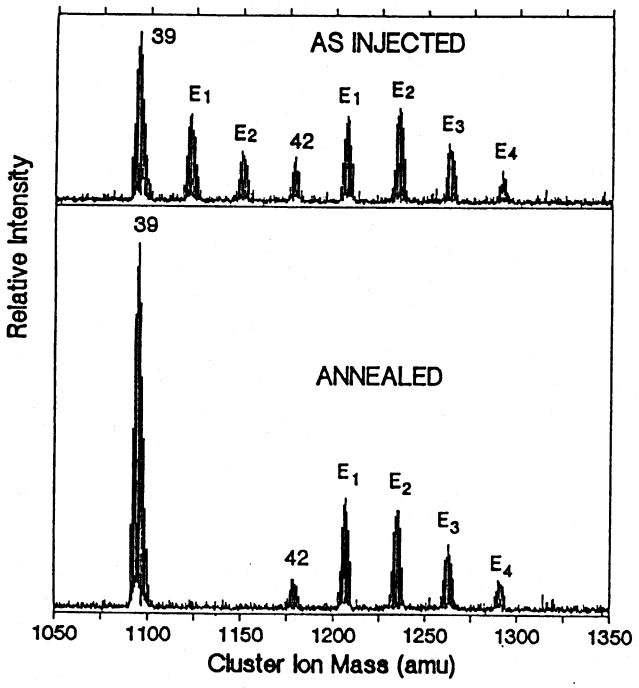

Fig. 6. Ethylene chemisorption study of Si_{39}^+ compared with Si_{42}^+ [4]. All other clusters have been removed from the ICR trap for clarity. Top panel shows the results of exposure to ethylene; bottom panel shows the same reaction study after annealing these clusters.

considerable reaction has occurred even for these "special" clusters. It was shown that much of this reactivity appears to be due to the presence of geometrical isomers of these special clusters, and to a great extent these reactive isomers may be "titrated" away [3].

However, the bottom panel of Fig. 5 (d) now demonstrates a more significant point: these reactive isomers of the special clusters 39, 45, and 48 atoms also turned out to be less stable energetically, and they can be annealed into the unreactive form by laser excitation. The panel (d) shows the result of reaction with ethylene just as in panel (c), except now the clusters had been irradiated with 30 pulses of light from a XeCl excimer laser (photon energy 4.0 eV) at a fluence of 1 mJ/cm^2 per pulse, and then allowed to cool with an additional 3 second, 2000 collision thermalization period with argon. Note that the reactivity of the clusters with 39, 45, and 48 atoms has been sharply reduced by this laser treatment, while the clusters with 36, 42, and 51 silicon atoms appear to be even more reactive. In fact, careful examination of the isotopic widths of the reaction products near Si_{39}^+ and Si_{45}^+ reveals that the majority of these reaction product is actually the result of multiple chemisorptions on smaller clusters.

Fig.6 further illustrate this point. In this case all injected ions except 39 and 42 were SWIFTed out from the cell. The top panel shows the reaction with ethylene after 5000 collisions. Again it is evident that, as injected, both clusters have a considerable fractional population of various reactive clusters. However the lower panel reveals that there is in fact a tremendous difference in the annealed forms of these two clusters. The annealed Si_{42}^+ remained highly reactive, while the annealed Si_{39}^+ displayed no evidence of any reaction at all.

A particular significant aspect to the top and bottom panels of Fig. 6 is that they have the same vertical scale factor. The markedly higher apparent intensity of the unreactive Si_{39}^+ in the bottom panel therefore is real: the reactive forms initially present for this cluster size have been efficiently converted into the unreactive form by the laser treatment. It is therefore certain that the dominant effect of the laser treatment is, in fact, annealing.

Magic numbers of 39 and 45 atoms for annealed silicon clusters are further verified for positively and negatively charged states with the trimethyleamine (TMA) reaction studies [5]. These results strongly support the idea that these annealed magic numbered clusters arrange themselves into unique geometrical structures.

5. METAL CLUSTERS

One of the most interesting results of transition metal cluster experiments is the existence of multiple isomers. FT-ICR experiments showed clearly that both Nb_{19}^+ and Ta_{10}^+ have at least two structural isomers with vastly different reactivities toward H_2 [6]. Here, the annealing technique verified for silicon clusters is applied to these metal clusters [7].

Fig. 7 shows the results of a hydrogen chemisorption study on Ta_{10}^+ [7]. Prior to the reaction only Ta_{10}^+ is selected in the ICR trap. The left hand column of Fig. 7 shows the as-injected Ta_{10}^+ clusters after exposure to 2x10^{-6} Torr hydrogen gas for various time periods. Remarkably after 3 s of reaction two third of the clusters is titrated to $Ta_{10}H_{18}^+$ and the other one third of clusters does not react at all even after 6 s reaction time. It is the clearest demonstration of existence of two isomers, one is reactive and another

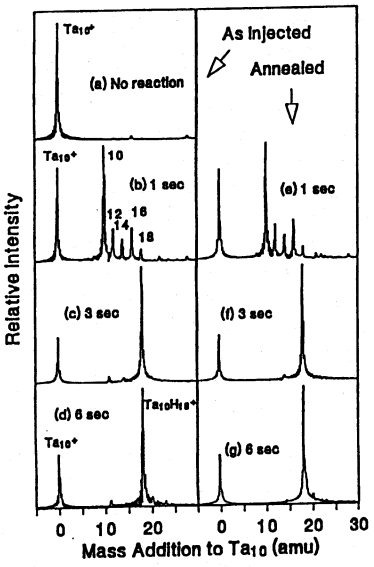

Fig. 7. Hydrogen gas chemisorption study on Ta_{10}^+ [7]. Exposure to 2x10^{-6} Torr hydrogen gas for labeled time period. (a)-(d) No annealing before reaction. (e)-(g) Laser annealing treatment prior to reaction.

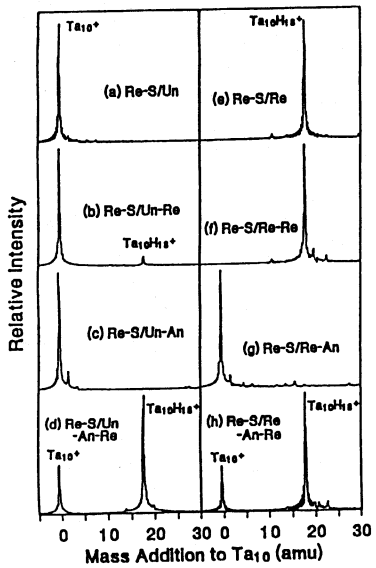

Fig. 8. Hydrogen gas chemisorption on selected unreactive or reactive Ta_{10}^+ clusters [7]. Panels on left hand column are results of selected unreactive clusters and panels on right hand column correspond to reactive clusters. (a) After removal of reactive clusters from Fig. 7 (c) (selection of unreactive clusters Ta_{10}^+). (b) 3 s exposure to H_2 on unreactive clusters. (c) Annealing treatment on unreactive clusters. (d) 3 sec exposure to 2x10^{-6} Torr H_2 after (c). (e) After removal of unreactive clusters from Fig. 7 (c) (selection of titrated reactive clusters $Ta_{10}H_{18}^+$). (f) 3 s exposure to H_2 on $Ta_{10}H_{18}^+$. (g) Annealing treatment on $Ta_{10}H_{18}^+$; H_2 are dissociated from Ta_{10}^+. (h) 3 s exposure to H_2 after (g).

is unreactive. Corresponding panels on the right hand column are results of the same reaction experiments as on the left hand column except that the laser annealing was performed prior to the reaction. In this case, however, practically no effect of annealing is observed.

Fig. 8 shows the results of an experiment designed to demonstrate that the laser annealing is in fact effective and can be used to interconvert the two forms of these tantalum clusters [7]. As shown in Fig. 7 (c), when Ta_{10}^+ clusters were allowed to react 3 s with H_2, reactive and unreactive isomers are completely separated to Ta_{10}^+ and $Ta_{10}H_{18}^+$. First, $Ta_{10}H_{18}^+$ clusters were ejected away from the ICR trap using the SWIFT leaving behind only the unreactive Ta_{10}^+ clusters (Fig. 8 (a)). These clusters were then exposed to hydrogen gas for 3 more second to make sure that they really are unreactive (Fig. 8 (b)). Fig. 8 (c) is the result when the clusters were annealed immediately after the selection of unreactive. Finally, the unreactive clusters are annealed and again exposed to hydrogen gas in Fig. 8 (d). Now, once again, one third of the clusters are found to be unreactive, the rest being converted into the reactive form.

The same series of experiments were repeated in Fig. 8 (e)–(h) where the unreactive form was ejected away and the reactive form ($Ta_{10}H_{18}^+$) was selected to be annealed. And, again the results is the same: the final ratio of the unreactive and reactive clusters is independent of the ratio before the annealing, 1:2.

As a final demonstration of the effect of annealing, Fig. 9 shows experiments where Ta_{10}^+ and Ta_{12}^+ clusters were exposed to $3x10^{-6}$ Torr N_2 [7]. The other clusters injected into the ICR cell at the same time were ejected away. The left hand column of Fig. 9 shows the reaction results without annealing and the right hand column after annealing. Using a different gas, it is again confirmed from Fig. 9 (d) and (h) that laser annealing has little influence on

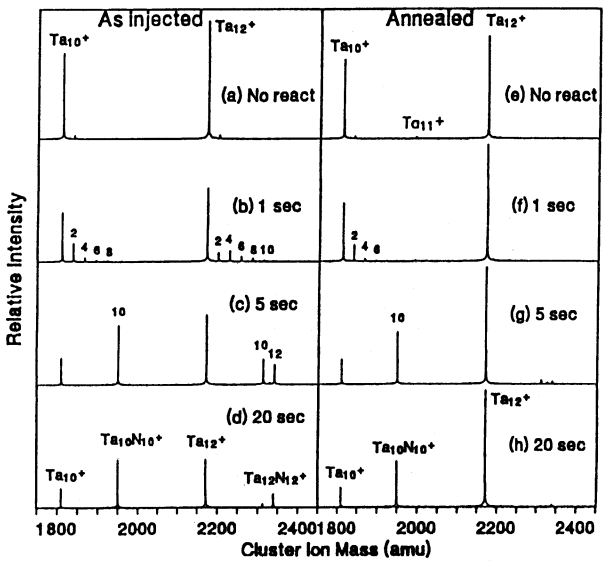

Fig. 9. Nitrogen gas chemisorption on Ta_{10}^+ and Ta_{12}^+ clusters [7]. All other clusters are removed. Exposure to $3x10^{-6}$ Torr nitrogen gas for labeled time period. (a)–(d) No annealing treatment. (e)–(h) Laser annealing prior to the reaction.

the reactivity of Ta_{10}^+. However, laser annealing has made a considerable difference with the Ta_{12}^+ clusters. Even though they appeared to have substantial component of reactive forms as they were initially injected into the ICR cell, laser annealing in this case has transformed all Ta_{12}^+ clusters into a single form which appears totally unreactive toward nitrogen gas under these conditions.

It sounds likely that the unreactive clusters are also energetically more stable compared with reactive ones. This assumption holds for silicon clusters of medium size range and Ta_{12}^+ clusters. Exceptions were Ta_{10}^+ and Nb_{19}^+ where unreactive and reactive forms have similar stability [7].

6. CARBON CLUSTERS AND FULLERENES

Carbon clusters are definitely special. Buckminsterfullerene (C_{60}) has been attracting many researchers since it was discovered to have the highly symmetric icosahidral structure [8] as shown in Fig. 10. Especially, since the macroscopic generation [9,10] and isolation of C_{60} were discovered, many possible applications like superconductivity have been sought [11].

Through the gas phase experiments of fullerenes, the FT-ICR apparatus with supersonic nozzle source had been proved to be a promising technique of studying extremely high mass range with high mass resolution. FT-ICR apparatus played a crucial role when the fullerenes with metals inside the cage were proved [12].

Another example is the following prove of giant fullerenes [13]. Fig. 11 shows the principal results. The top panel (a) is the FT-ICR mass spectrum obtained after SWIFTing out all clusters except those in the range between C_{288}^+ and C_{316}^+. Note that the detection technique also picks up a bit of signal at the 2nd and 3rd harmonic of the fundamental cyclotron motion of the cluster ions in the trap. This makes each peak in the mass spectrum reappear with much reduced intensity at an apparent mass 1/2 and 1/3 of the true mass, respectively.

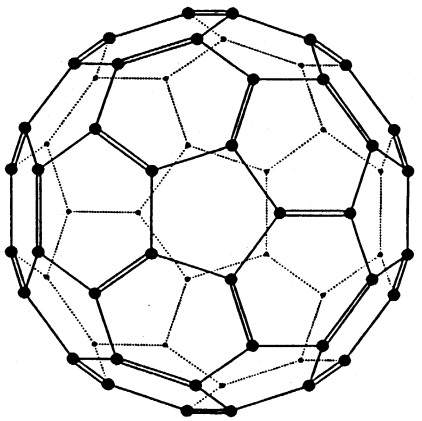

Fig. 10 Structure of Buckminsterfullerene (C_{60}). Carbon atoms are at the vertices of the truncated icosahidron. Bonds between adjacent hexagons are double bonds and others are single bonds.

Note that the mass spectrum in this region consists primarily of just even-numbered carbon clusters. O'Brien et al. [14] found that (C_{60}^+) was extremely resistant to photofragmentation, but ultimately it does fragment by the loss of even numbered small carbon radicals. Here now in Fig. 11 we see the carbon clusters in the size range of 288-316 also fragment by the loss of even-numbered fragments. The middle panel of Fig. 11 (b) shows the result of an equivalent experiments to that of Fig. 11(a), except that at the end the clusters were irradiated with 100 shots of a XeCl excimer laser beam (4.0 eV) at a fluence of 35 mJ/cm^2 per shot over a time period of 2 seconds. This high level of laser fluence through the ICR cell was permissible only because the front and back door electrodes of the cell had 2.5 cm diameter open holes along the central axis without any obstructing grids. This laser exposure was chosen to show the photofragment distribution pushed down to the region near C_{150}^+. Lower level of laser excitation were found to produce correspondingly less extensive fragmentation, with the fragment size distribution concentrated near the parent clusters.

Results similar to these have been obtained for all fullerenes in the size range from 150 through 600 atoms. All appear to fragment simply by C_2 and larger even-numbered carbon radical loss.

The FT-ICR spectrum of Fig.11 (b) in the relatively small mass region (80-150) is one of the most interesting aspect of this data. Note that here there appeared to be both odd and even-numbered clusters. Of course, in this region there is some interference from the second harmonic of the ICR signal of the clusters in the 160-300 size region as quite evident in Fig. 11 (a). However, this second harmonic interference cannot explain all the observed apparent "odd" carbon fragment clusters seen in Fig. 11 (b). This is proven in the bottom Fig. 11 (c) which is the mass spectrum detected after all clusters larger than C_{252}^+ were SWIFTed. Now there is negligible interference from harmonics of higher mass clusters. But, still there are the "odd" peaks.

Fig. 12 shows an expanded mass scale version of this same mass spectrum (the same as Fig. 11 (c)). The top panel shows the mass spectrum in the region corresponding to C_{112}^+ to C_{120}^+. Note that clear isotopic substructure. Each fine structure peak is found to be separated from the next by an apparent 0.5 amu interval. These are, therefore, not due to odd-numbered carbon clusters whose substructure should have 1 amu separations as expected from the 1.11 % natural abundance of ^{13}C. Instead they are due to even-numbered but doubly charged clusters, as labeled in the figure. They have been generated here by laser excitation of singly-charged fullerenes in the 288-316 size range.

The lower panel of Fig. 12 shows an expanded view of the mass spectrum of Fig. 11(c) in the C_{152}^+ to C_{160}^+ size range which is right at the onset of the laser induced doubly-charged fragment distribution. Note that the interval of the isotopic substructure peaks in clearly 1 amu for the even-numbered clusters in this size range. They are therefore, the singly-charged fragments as labeled in Fig. 12.

When clusters are levitated in the high vacuum of ICR trap and excited at high levels, ordinally, they simply fragment to cool down. A fullerene in the size range of 300 atoms, however, is believed to have a stable large hollow cage structure, and the second ionization potential should not be more than a few eV higher than the first. There are 300 pi electrons delocalized around the surface of this hollow object. And, fullerenes with the closed cage structure are expected to have long life time at a high temperature until the coupling vibrational energy into a single electron to let it boil off. Therefore, the thermionic emission, which is familiar for very hot macroscopic objects, can be a reasonable explanation of this +2 charged fullerenes.

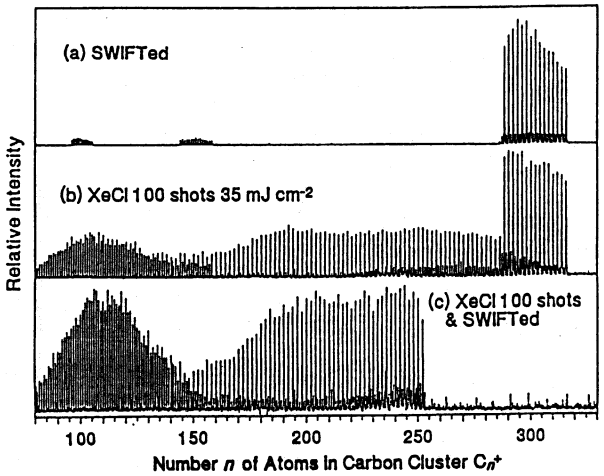

Fig. 11. Photofragmentation and multiple ionization of giant fullerenes C_{288}^+ to C_{316}^+ [13]. (a) All clusters except for C_{288}^+ through C_{316}^+ are removed by "SWIFT". (b) After irradiation with 100 shots of a XeCl excimer laser at a fluence of 35 mJ/cm^2. (c) The same condition as (b) except that all clusters larger than C_{252}^+ are swept from the ICR trap prior to detection in order to remove the interference from 2nd harmonic detection of larger clusters.

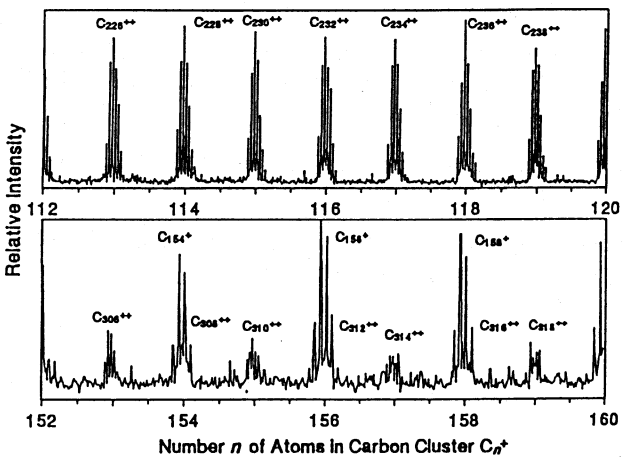

Fig. 12. Expanded mass scale of FT-ICR spectrum shown in Fig. 11 (c) [13]. Note that isotopic substructure of the peaks in the top panel appears to be spaced at 0.5 amu intervals. This proves that they are due to clusters with a charge of +2.

7. CONCLUDING REMARKS

I would like to remark that this paper is a summary of FT-ICR studies performed and published with professor R. E. Smalley and his students, L. R. Anderson, T. Guo, M. Y. Lee, C. Chen, R. T. Laaksonen, R. E. Haufler, and Y. Chai, at Rice Quantum Institute and the Departments of Chemistry and Physics, Rice University, while I was visiting Rice University from May 1989 through February 1991.

REFERENCES

(1) Maruyama, S., Anderson, L. R. and Smalley, R. E.: Rev. Sci. Instrum., 61, 3686 (1990).

(2) Alford, J. M., Laaksonen, R. T. and Smalley, R. E.: J. Chem. Phys., 94, 2618 (1991).

(3) Anderson, L. R., Maruyama, S. and Smalley, R. E.: Chem. Phys. Lett., 176, 348 (1991).

(4) Maruyama, S., Anderson, L. R. and Smalley, R. E.: J. Chem. Phys., 93, 5349 (1990).

(5) Maruyama, S., Anderson, L. R. and Smalley, R. E.: Mat. Res. Soc. Symp. Proc., 206, 63 (1991).

(6) Laaksonen, R. T., Elkind, J. L., Weiss, F. D., Alford, J. M. and Smalley, R. E.: J. Chem. Phys., submitted (1991).

(7) Maruyama, S., Guo, T., Chen, C., Laaksonen, R. T. and Smalley, R. E.: Chem. Phys. Lett., submitted (1991).

(8) Kroto, H. W, Heath, J. R., O'Brien, S. C., Curl, R. F and Smalley, R. E.: Nature, 318, 162 (1985).

(9) Krätschmer, W, Lamb, L. D., Fostiropoulos, K. and Huffman, D. R.: Nature, 347, 354 (1990).

(10) Haufler, R. E., Chai, Y., Chibante, L. P. F., Conceicao, J., Jin, C., Wang, L.-S., Maruyama, S. and Smalley, R. E.: Mat. Res. Soc. Symp. Proc., 206, 63 (1991).

(11) Maruyama, S.: NEW DIAMOND, 24, 32 (1992).

(12) Chai, Y., Guo, T., Jin, C, Haufler, R. E., Chibante, L. P. F., Fure, J., Wang, L., Alford, J. M. and Smalley, R. E.: J. Phys. Chem., 95, 7564 (1991).

(13) Maruyama, S., Lee, M. Y., Haufler, R. E., Chai, Y. and Smalley, R. E.: Z. Phys. D, 19, 409 (1991).

(14) O'Brien, S. C., Heath, J. R., Curl, R. F. and Smalley, R. E.: J. Chem. Phys., 88, 220 (1988).